PERIODICO di MINERALOGIA
established in 1930

DIPARTIMENTO DI SCIENZE DELLA TERRA
SAPIENZA UNIVERSITÀ DI ROMA

An International Journal of
Mineralogy, Crystallography, Geochemistry,
Ore Deposits, Petrology, Volcanology
and applied topics on Environment, Archaeometry and Cultural Heritage

Soil geochemistry survey for gold exploration at Kısacık area (Çanakkale, Ayvacık, Türkiye)

Alaaddin Vural *

Ankara University, Faculty of Engineering, Department of Geological Engineering, 50.Yıl Yerleşkesi 06830 Gölbaşı, Türkiye

ARTICLE INFO

Submitted: December 2023
Accepted: May 2024
Available on line: May 2024

* Corresponding author:
alaaddinvural@hotmail.com

Doi: 10.13133/2239-1002/18335

How to cite this article:
Vural A. (2024)
Period. Mineral. 93, 61-83

ABSTRACT

The Kısacık gold deposit (Çanakkale, Türkiye) is a recently discovered area identified through soil geochemistry studies. Soil geochemistry surveys in the region commonly employed high detection limits for gold (40 ppb) and silver (5 ppm). Despite this disadvantage, a significant gold mineralization was discovered at the Kısacık site. This study has two main goals: establishing reliable threshold values for analyzed elements with high detection limits, and determining if the multi-element halo technique can reveal subtle anomalies that may be missed using single-element mapping. For this purpose, a total of 305 surface-soil samples collected from the area were investigated for the concentration and spatial distribution of gold and its seven pathfinder elements (Cu, Pb, Zn, As, Mo, Sb, and Ag). Frequency-based conventional methods and fractal/multifractal-based concentration-number (C-N) method were used to calculate the threshold values, and robust threshold values were obtained with the C-N method. To prepare the distribution of element concentrations on a contour map, the data were used to calculate the variograms (ordinary Kriging prediction) of elements in soil in the area for spatial prediction. When the single element anomaly maps of all elements were assessed, no sufficient surface enrichment/anomaly halos were seen in the area. To enhance the data, the multi-element halo technique was used to create an anomaly map. From the anomaly maps formed via the multi-element halo technique, it can clearly be seen that they are an improvement on the single-element anomaly maps. Consequently, the multi-element halo technique seems to be more efficient in the assessment of vulnerable (weak) data and insufficient geochemical anomalies for geochemical explorations.

Keywords: C-N fractal method; single element/multielement halos; iso-concentration mapping; soil geochemistry; gold exploration.

INTRODUCTION

The element content of soils and their behavior patterns have been the subject of many studies for different purposes (Carranza, 2009a; Gerla et al., 2011; Drewnik et al., 2014; Sungur et al., 2015; Alfaro et al., 2018; Vural, 2019, 2020) but has a low threshold for toxic concentration. It is recommended that nutrients such as Se should be consumed through foods as part of a normal diet. Se concentrations in crops and meat depend on the amount of labile Se in the soil where crops and forage are grown. Therefore, managing agriculture for optimal Se in grain crops and forage requires an understanding of the distribution and mobility of Se. Elevated concentrations of Se occur in waters, soils, and forage 120 km west of Pierre in west central South Dakota, USA. The research site lies in an elevated, dissected plain where soils developed on gently dipping Pierre Shale. Soils were sampled along catena transects and waters collected from soil, ponds, and shallow borings in areas of known elevated forage and crop Se. Soil extracts from saturated-paste extraction and acid

(aqua regia and hydrofluoric acid. There are many studies focused on soil quality, pollution of agricultural soils, and heavy metal pollution in the years after 1980 when environmental awareness and sustainable development facts gained importance (Esmaeili et al., 2014; Sungur et al., 2014; Shi et al., 2018; Sosa-Rodríguez et al., 2020) mining and industrial discordant development over the last several decades, which has jeopardized the ecology, food safety, human health, and sustainable development of agriculture. To investigate the soil pollution, a total of 105 agricultural soil samples and 40 background soil samples were collected from the Isfahan industrial zone. Accordingly, total concentrations of 7 heavy metals (including Cu, Pb, Zn, Cd, Ni, Co and Cr. However, the first and most important studies for soil geochemistry are exploration geochemistry studies (Mazzucchelli, 1996; Yusta et al., 1998; Yilmaz, 2003) suggesting Ag-poor Pb-Zn mineralization, whereas the ratio at Turkmen is extremely high (maximum 86. With these studies, many mineral deposits were found and brought to the economy also (Vural, 2006; Vural and Aydal, 2020a). Nowadays, there are mostly studies on natural or geological origin (hydrothermal alteration, weathering, thermal spring, etc.) element enrichments in the soil (Vural, 2015a; Vural and Çiçek, 2019, 2020). Many analytical and statistical methods are also used in soil geochemistry studies (Reimann et al., 2002; Sany et al., 2011; Wang et al., 2013; Machender et al., 2014; Sadeghi et al., 2014; Carranza, 2017; Xiong et al., 2018; Ahmadfaraj et al., 2019; Ghezelbash et al., 2019; Xu et al., 2020; Zhang et al., 2021).

Gold is a relatively immobile element in superficial environments, especially in arid/semiarid climatic conditions (Reis et al., 2001; Vural, 2006; Aydal et al., 2007). For this reason, the geochemically superficial anomaly of a gold enrichment area is often limited and/or difficult to detect or interpret. However, under certain physical and chemical conditions, epigenetic gold may become mobile and disperse from its source to form geochemical gold anomalies at the surface (Reis et al., 2001; Vural, 2006, 2019; Vural and Aydal, 2020a). Soil geochemistry studies in the exploration of gold are indispensable and one of the most important processes in this field. However, both adversities during the sampling and methods used in the analysis of samples make the exploration of gold difficult. In addition, the physical and chemical properties of gold offer poor sample representativity, such as malleable particles, its being highly resistant to comminution (depending on its occurrence in the cage system of minerals, especially in epithermal mineralization), and a poor analytical method (Nichol et al., 1989; Reis et al., 2001; Vural and Aydal, 2020a). The way to overcome such problems, besides using large amounts of the sample for analysis, is the use of appropriate analytical methods and procedures. Moreover, the data obtained must be evaluated properly, especially at the stage of determining the threshold value (Bounessah and Atkin, 2003; Bech et al., 2008; Chen et al., 2019) Ni, and Cu in the soils of Barcelona Province (NE Spain).

In this study, the behavior and spatial distribution characteristics of gold and related trace elements in the soil at Kısacık (Ayvacık-Çanakkale, NW Türkiye) which is also a mineralization area (gold deposit), were comparatively performed using classical method (such as mean±2standart deviation, histogram, and cumulative frequency curves, medyan±2medyan absolute deviation, etc.) and concentration-area fractal method for calculating the threshold values, and single element and multi-element halo method for iso-concentration mapping.

The aim of the study is to examine the gold enrichment in the Kısacık area using various statistical methods and single-element and multi-element halo mapping techniques, using the results of soil geochemistry analyses that can be considered vulnerable (weak) because the data used in the study is <80 mesh depending on the working process of the Institution (General Directorate Mineral Research and Exploration, MTA in Turkish abbreviation) and the data measured with atomic absorption with 40 mg/kg detection limit for gold and 5 mg/kg detection limit for silver). The Kısacık gold mineralization area is situated at Ayvacık-Çanakkale, Biga Peninsula, Northwest Anatolia. The Biga Peninsula, in terms of ore deposits, has known since antiquity and has had many of its deposits exploited (Vural et al., 2009) and the region is an important metallogenic region containing various mineralizations, such as copper, lead, zinc, iron, gold, tungsten, molybdenum, antimony, mercury, etc., from different ages and phases of granite intrusions and volcanic activities that have created various types of mineralization. Therefore, the geology and mineralization of the region have always attracted the attention of many researchers, and there are many such studies on the region (Bingöl, 1975; Okay et al., 1996; Genç, 1998; Karacık and Yılmaz, 1998; Okay and Satir, 2000; Dönmez et al., 2005; Aydal et al., 2006a, 2006b; Vural, 2006; Vural et al., 2011; Vural and Aydal, 2020b, 2016).

During prospecting surveys carried out in the 1990s and between 1998 to 2005 by MTA in the region, especially in Kısacık village and its surrounding areas, it was determined to be a place of intense alteration, appropriate structural conditions, and acidic intrusions, indicating the potential of gold mineralization, such as epithermal gold deposits.

Geological setting

Kısacık gold area is located in the Biga peninsula, Western Anatolia, Türkiye. Pre-Tertiary, Tertiary and Post

Tertiary Units are situated in the study area and its near vicinity (Okay et al., 1990; Vural, 2006; Aydal et al., 2007; Vural and Aydal, 2020a). Pre-Tertiary units were divided into three tectonic units by Okay et al. (1990): from NW to SE, the Sakarya Zone, the Ayvacık-Karabiga Zone, and the Ezine Zone. The Sakarya Tectonic Zone mainly consists of the Kazdağ group metamorphic rocks and the Karakaya Complex (Bingöl, 1975; Duru et al., 2004; Okay and Altiner, 2004; Okay and Göncüoğlu, 2004) which overlaid these metamorphic and Post-Triassic sediments. The Ayvacık-Karabiga Zone consists of an ophiolitic mélange (Çetmi ophiolitic mélange). Eclogite blocks and Upper Triassic limestone blocks belonging to the mélange are characteristic of the Ayvacık-Karabiga Zone. The Ezine Zone consists of continental-originated rocks. This zone consists of a Permo-Carboniferous sedimentary sequence (Karadag Unit), which was metamorphosed at green schist facies, and an ophiolite (Denizgören ophiolite) which overlaid this sedimentary sequence in the Permo-Triassic period in the west. It also consists of sedimentary-originated high-grade metamorphic rocks (Çamlıca Micaschist) (Okay et al., 1990; Vural, 2006; Vural and Aydal, 2020a). In the region, Tertiary and Post-Tertiary units began with middle Eocene neritic limestone and Upper Eocene turbidities, interbedded andesite, and andesitic tuff, which concordantly overlaid the neritic limestone. Then, with the disconformity plane, Eocene (?)/ Oligo-Miocene calc- alkaline magmatism was influential in the region (Siyako et al., 1989; Okay et al., 1990; Genç, 1998; Okay and Satir, 2000; Dönmez et al., 2005). Dacite, andesite, rhyolite, and acidic tuffs, as lateral transitions with sedimentary rocks containing coal in some places, are exposed (Vural, 2006; Altunkaynak and Genç, 2008).

In the study area, Tertiary/Post-Tertiary units are composed of magmatic and sedimentary rocks (Figure 1). Magmatic rocks span the Eocene (?)/Oligocene to the Upper Pliocene- Quaternary (?) aged and they are composed of plutonic and volcanic rocks and their pyroclastics (Aydal et al., 2006b; Vural, 2006; Vural and Aydal, 2016), sedimentary rocks, aged Upper Miocene-Pliocene areas, mostly composed of lacustrine and terrestrial clastics, and Quaternary alluvium.

Plutonic rocks can be seen outside of the study area, in the northern. Volcanic rocks (Alakeçi-Kısacık Volcanics, Vural, 2006) in the area are alterated (hematitized and silicified), and mostly consist of andesite, latites, rhyolite, basaltic andesite, ignimbrite, basaltic trachyandesite lavas and pyroclastic rocks. These rocks are lateral passes with fluvial conglomerates and lacustrine sedimentary rocks. These rocks were dated as belonging to the Early-Middle Miocene period by Siyako et al. (1989) and Genç (1998). The latest product of magmatism, basalt lava, can be seen in the western vicinity of the area.

The study area lies within a region of volcanic rocks intruded by thin silica veins. This area, near Kısacık-Kırantepe, exhibits intense silicification and hematite coating, suggesting potential for gold mineralization. The author's PhD research for the MTA project included soil geochemistry exploration in this very area. Although gold minerals were not detected in the results of the ore microscopy studies, remarkable gold concentrations were detected by geochemical analysis and that a small amount of gold grains were seen in the gold pan.

MATERIAL AND METHODS

For the determination and examination of mineralization in the area, 305 soil samples were collected in a rectilinear grid at equal distances (50 m) along evenly spaced lines (50 m). The lines were oriented perpendicularly to the NE-SW trending alteration zone (Figure 1).

The samples, collected from the B zone of the soil layers at 30-35 cm depth, were dried at a temperature of 60°C for 24 h. A <80 mesh fraction obtained by dry sieving was retained for chemical analysis. Samples were analyzed at a laboratory of MTA (LOMTA) for Ag, As, Mo, Sb, Cu, Pb, and Zn via a flame atomic absorption spectrometer, Shimadzu AA-680 FAAS with single element hollow cathode lamb, and, due to the gold value in the soil being low, gold analysis were conducted by graphite-furnace atomic absorption (GFAAS). LOMTA's procedures were applied during the analysis. Standards (LOMTA's standards) were also used during the analytical processing of the elements. The process is briefly as follows (also see Vural and Aydal (2020a)):

- A series of mixed standard solutions containing each metal ion were prepared from stock metal solutions.
- The solutions were introduced to the instrument to plot calibration charts.
- The soil samples were finally taken into solution form after being digested with aqua regia reagent (3:1 ratio conc. HCl and HNO_3) were measured in the device, and concentrations of the solutions containing each metal ion were determined via relevant calibration charts.

The concentrations measured in mg L^{-1} (or μg L^{-1}) in solution were then converted to mg/kg (or mg/kg) by the following formula 1:

$$Concentration\ (mg/kg\ or\ \mu g/kg) = \frac{C \cdot V \cdot D}{m} \qquad 1)$$

C: The concentration value of mg/L or μg/L measured in aqueous solution by AAS

V: Final volume (mL) after being digested the samples with aqua regia

m: Weighed sample mass (g)

D: Dilution coefficient

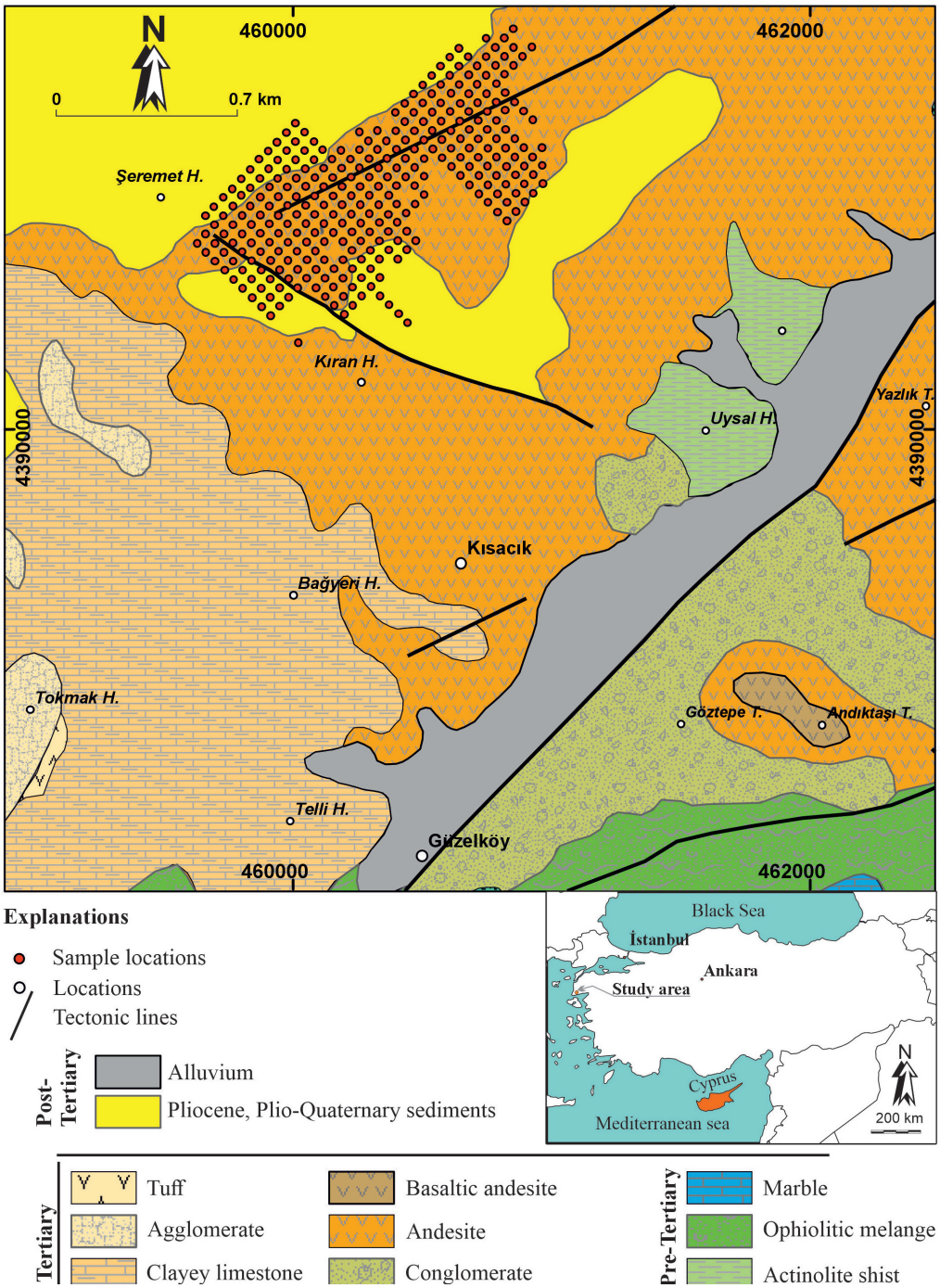

Figure 1. Geological map of the study area [After 15] and sampling locations.

Accuracy and sensitivity tests of sample analysis were performed according to Skoog et al. (2004):

The method accuracy was verified by a certified reference material, CRM-SA-C-Sandy Soil C. The method, aqua regia wet digestion-AAS determination, was applied to CRM and the results are given in Table 1. As shown in the table, the recoveries are quite satisfactory. The results of the *t*-test on whether the certified value and the obtained value are close to each other, are also quite satisfactory. Precision of the method was evaluated with relative standard deviation (RSD). The solution containing the corresponding metals at a concentration

Table 1. Analysis results of a certified reference material, CRM-SA-C-Sandy Soil C, for accuracy of the method (N=3), (All elements in mg/kg).

	X_{CRM}	S_{CRM}	X_F	s_F	*R (%)*	*E (%)*	*RSD (%)*	X_F-X_{CRM}	*Sf/√N*	t_c	$t_{critical}$*	*Comparison*
Co	12.4	0.6	11.7	0.8	94.0	-6.0	6.6	-0.750	0.445	-1.69	4.30	Same
Ni	48.4	3.0	44.4	2.9	91.8	-8.2	6.6	-3.960	1.686	-2.35	4.30	Same
Cu	63.6	4.0	61.2	3.2	96.2	-3.8	5.2	-2.400	1.848	-1.30	4.30	Same
Zn	607.0	30.0	575.0	34.0	94.7	-5.3	6.0	-32.400	19.780	-1.64	4.00	Same
As	67.7	4.2	60.7	4.2	89.6	-10.4	6.9	-7.040	2.425	-2.90	4.30	Same
Ag	24.6	1.6	22.3	1.4	90.8	-9.2	6.1	-2.270	0.785	-2.89	4.30	Same
Mo	53.6	4.0	47.8	3.6	89.1	-10.9	7.5	-5.830	2.078	-2.80	4.30	Same
Pb	120.0	8.0	114.2	3.4	95.2	-4.8	3.0	-5.780	1.986	-2.91	4.30	Same
Au	(25)**		21.0	2.0	84.9	-15.1	10.7	-3.780	1.305	-2.90	4.30	Same

Note: If $t_{cal} \geq t_{critical}$ or $t_{cal.} \leq -t_{critical}$, H_o (null hypothesis) is rejected. So, there is a statistically significant difference between the 2 results compared. $t_{cal.}$ is calculated by the following formula:

$$t_{cal.} = \frac{X_F - X_{CRM}}{s_F/\sqrt{N}}$$

* $t_{critical}$ value for p = 0.05
**The value given is for informational purposes, not certified.
X_{CRM}: Mean of the certified value
S_{CRM}: Standard deviation of the certified value
X_F: Mean of the found value
S_F: Standard deviation of the found value
R: Recovery
E: Error
RSD: Relative standard deviation
t_{cal}: Calculated *t* value
$t_{critical}$: Critical *t* value

of 0.1 mg/ L was analyzed 20 times by the same method. The standard deviation of the results was calculated and RSD% values were found for each metal with the following formula 2:

$$RSD\ (\%) = \frac{s}{\bar{X}} \cdot 100 \qquad 2)$$

RSD: Relative standard deviation
s: Standard deviation
$\bar{X}$: Mean value

LOD (limit of detection), which is the lowest concentration detected by the method, was calculated by taking three times the standard deviation of the results obtained after the analyses of 20 blank solutions. LOQ (limit of quantification), which is the lowest concentration detected quantitatively by the method, was calculated by taking 10 times the standard deviation of the results obtained after the analyses of 20 blank solutions. RSD, LOD and LOQ values of each metal are given in Table 2.

Table 2. Analytical figure of merit of the method.

	LOD		LOQ		RSD
	mg/L	mg/kg*	mg/L	mg/kg*	%
Co	15.00	1.500	50.0	5.00	1.4
Ni	15.00	1.500	50.0	5.00	1.3
Cu	10.00	1.000	33.0	3.30	2.1
Zn	10.00	1.000	33.0	3.30	2.6
As	20.00	2.000	66.0	6.60	1.7
Ag	0.10	1.000	33.0	3.30	2.1
Mo	15.00	1.500	50.0	5.00	1.2
Pb	25.00	2.500	83.0	8.30	3.2
Au**	0.13	0.013	0.4	0.04	2.2

*mg/kg LOD and mg/kg LOQ values were calculated by Formula 1.
**measured by graphite furnace AAS.

Data Analysis

In the first step of the study, the descriptive statistics, such as mean, geometric mean, median, minimum, maximum, variance, etc., and the correlation coefficient and normality tests (Kolmogorov-Smirnov and Shapiro-Wilk tests) for eight elements in the soil samples, were also determined (Table 3, 4 and 5). Neither factor analysis (Principal Component Analysis-PCA) nor staged factor analysis could be applied because the data were not suitable for factor analysis.

The second step was to estimate the threshold-background value of the elements. Many sophisticated methods such as correlation analysis, factor analysis, cluster analysis, fractal analysis, multifractal analysis, spatially weighted singularity mapping method are used to determine the background-threshold values, spatial distribution and patterns of the elements in the soil (Carranza et al., 2009; Carranza and Sadeghi, 2010; Agterberg, 2012; Wang et al., 2017, 2013; Meigoony et al., 2014; Yilmaz et al., 2015; Nazarpour et al., 2015; Afzal et al., 2016; Ghezelbash et al., 2019; Xu et al., 2020; Ayad and Bakkali, 2022; Ayad, 2023). Both geochemical and statistical methods are used to evaluate the background concentrations of elements in the soil. Statistical methods are more popular than geochemical methods. Because with these methods, not only anomalies and threshold values are determined, they also have low laboratory workload and costs (Esmaeili et al. 2014; Vural 2015a). In estimating the threshold value and background concentration, mean ±2*standard deviation has been used for almost 60 years for the normal dataset, and geometric-mean or median±2*standard deviation for lognormal dataset. These are conventional methods and frequency-based (Aitchison, 1986; Filzmoser and Hron, 2008). Also, percentiles have been used to define threshold values (Sinclair, 1974) as follows:

Threshold=Q_3+(Q_3-Q_1)*1.5; Q_3 and Q_1 are the 75th and 25th percentiles of the element concentrations respectively. However, the mentioned method was not used in calculating the threshold value in this study.

Another conventional technique for threshold values is the median ±2*Median Absolute Deviation (MAD), which is recommended for positive skewed dataset (Reimann et al., 2005; Teng et al., 2010; Vural, 2017) because the median value is generally less sensitive to outliers. MAD is calculated as follows (Hampel, 1974):

$$MAD= M_i(\lvert X_i-M_j(X_j)\rvert) \quad 3)$$

where M_i and M_j donate the median of the series i and j respectively, X_i donates each observation in the population and X_j represents original population.

Concepts related to natural processes and earth sciences operate in accordance with Fractal geometry rather than Euclidean geometry (Mandelbrot, 1983). Therefore, different fractal analysis approaches have been proposed since the 1980s, especially in geochemical exploration such as Number-Size [N-S: (Mandelbrot, 1983)], Concentration-Number [C-N: (Hassanpour and Afzal, 2013)], Concentration-Area [C-A: (Cheng et al., 1994)], Concentration-Distance [C-D: (Li et al., 2003)], Power Spectrum-Volume [S-V: (Afzal et al., 2012)], etc. Each of the methods has its advantages and disadvantages. The discussion of these methods and their comparison with each other are excluded from this article. Detailed discussions of them by various researchers are available in the literature (Reimann and Filzmoser, 2000; Carranza and Hale, 2001; Reis et al., 2001; Reimann et al., 2002; Vural, 2018, 2006, 2015c, 2015a, 2016; Carranza, 2009a; Carranza and Sadeghi, 2010; Xiong et al., 2018). One of the most widely used fractal analysis methods is the C-N modeling method. This fractal model which was first proposed by Mandelbrot (1983) is a subset of C-A and can be utilized easily to estimate the distribution characteristic of the geochemical population (both threshold and geochemical background) for raw data. The model is expressed by the following equation:

$$N(\geq\rho)\propto\rho^{-\beta} \quad 4)$$

where $N(\geq\rho)$ donates the number of the cumulative samples having concentrations equal to or higher than r which donates the element concentration, and β is the fractal dimension. This model is also rewritten as

$$Log[N(\geq\rho)]=-\beta log(\rho) \quad 5)$$

$N(\geq\rho)$ versus ρ log-log plot shows linear parts with different slopes which show -b values, representing different concentration ranges (Hassanpour and Afzal, 2013; Afzal et al., 2015).

Although very sophisticated statistical methods are used in soil geochemistry studies/exploration geochemistry, what is important is that the method works well. Therefore, it is the final result that the methods used are expected to be verifiable. The findings obtained statistically in this study had the opportunity to be controlled by drilling in the field. In this study, the mean plus two standard deviations (with the help of histogram and cumulative frequency curves; for both normal and nonnormal distributions) method and the median plus two MAD method (MMAD), from the conventional methods (Equation 3), and the Concentration-Number (C-N) fractal method (Equation 4 and 5) from nonconventional methods were used to estimate the threshold values of the elements (Figure 2, 3 and 5). Concentrations corresponding to approximately

95.44% on the cumulative frequency curves on histogram versus cumulative frequency plots were accepted as the threshold value of the elements (Figure 2, Table 3). Obtained threshold values were also compared with their upper crust values according to Rudnick and Gao (2010) (Table 3).

In order to enhance the superficial geochemical signature of gold and its pathfinders, a comparative study was carried out using different mapping techniques such as iso-concentration single-element mapping based on classical approaches and multi-element halo techniques, which were explained in detail by Reis et al. (Reis et al., 2001). Thus, in the next step of the study, iso-concentration single-element distribution maps were plotted for each element, and by using the threshold values, the distribution characteristics of the elements in the field and the gold enrichment areas were examined (Figure 4). Subsequently, multi element haloes maps were plotted (Figure 6) considering the correlation relationships between the elements and gold and the results of iso-concentration single-element distribution maps and multi element haloes maps were compared. In this paper, gold-related elements in the literature, such as Ag. As, Mo, Sb, Cu, Pb, Zn, etc., and the chemical elements strongly correlated with gold were primarily studied (Reis et al., 2001; Anand et al., 2019). Since there was a high detection limit in the analysis of the elements used in the study, the data were evaluated using empirical approaches in some parts. Evaluation of the data was attempted as efficiently as possible. All data were evaluated with the SPSS 25 statistical software package, Microsoft Excel and ArcMap 10.5 software.

RESULTS

Descriptive statistics and correlation coefficients

Element concentrations of soil samples from the study site were evaluated using descriptive statistics' parameters, and these parameters (mean, geometric mean, median, minimum, maximum, variance, etc.) of the 305 soil samples are listed in Table 3. The average values of elements in the continental crust, suggested by Rudnick and Gao (2010) were considered as background values in this study. Almost all element concentrations in the area were found to be higher than the background values (Table 3). The minimum and maximum with their arithmetic means of Cu, Pb, Zn, As, Mo, Sb, Ag and Au concentrations in the site are (in mg/kg, except Au); 5 to 57 with 18.97; 10 to 118 with 24.42; 5 to 97 with 31.93; 20 to 780 with 129.36; 5 to 2950 with 218.01; 10 to 54 with 19.70; 5 to 40 with 8.71 and 40 to 8200 with 350.66 (in mg/kg) respectively. It was clear that the median values of all elements investigated were less than their arithmetic means, and geometric means are close to the median of the elements, but they are usually slightly higher. (Table 3). As indicated (see Table 3) by their standard deviations and skewness coefficients (for raw data), all distributions of the elements are positively skewed (also see Table 4).

Some maximum values are very high, over three to 10 standard deviations from the means of elements. While extreme values were omitted from the data set in the graphical threshold estimates (Figure 2), operations were performed without omitting them in other processes since some of the anomalies could be signal for potentially buried mineralization. Because the datasets have positive skewness, and so, are due to have a logarithmic distribution, a decimal logarithmic of the data of the Kısacık area was used in all processes instead of raw data, which very effectively reduces the asymmetry of the distribution (although the data could not be converted to an ideal gaussian distribution by any method tried), as testified by the skewness coefficient and normality tests.

Considering that soil element concentrations were mostly not normally distributed, a Spearman Correlation (SC) matrix was calculated instead of a Pearson Correlation (PC) matrix to determine the correlation between elements. It was earned out using the Spearman rank sum method, as it is nonparametric, less sensitive to outliers and does not assume a linear relationship between variables. The SC matrix is presented in Table 5. It was hoped that the obtained correlation matrix provides clues about the pathfinder element association with gold. According to the SC matrix, Cu shows a strong correlation with Zn (0.75). Pb shows a weak correlation with Sb (0.56) and a moderate to strong correlation with As (0.67). As shows a weak to moderate correlation with Sb (0.54). A strong correlation between Mo and As (1.00) according to the SC coefficient is evident, but this is a fairly suspicious outcome due to insufficient data for those elements. No significant correlation was observed between Au, Ag, and the other elements examined (except between Au and Sb). The GFAAS method was used for gold and silver in the soil geochemistry study. As is known, it is not possible to achieve low detection limits for trace elements such as Au and Ag with the GFAAS method. Working with high detection limits compared to background values for such trace elements can potentially mask correlations between elements. However, as the relationships among the elements examined were considered, also by using the literature (e.g. Darwish and Poellmann, 2010; Anand et al., 2019), the elements examined in the investigation of gold enrichment in the study field were accepted as pathfinder elements.

The threshold values

Frequency/percentage distribution graphs were created for the elements, both raw data and logarithmically

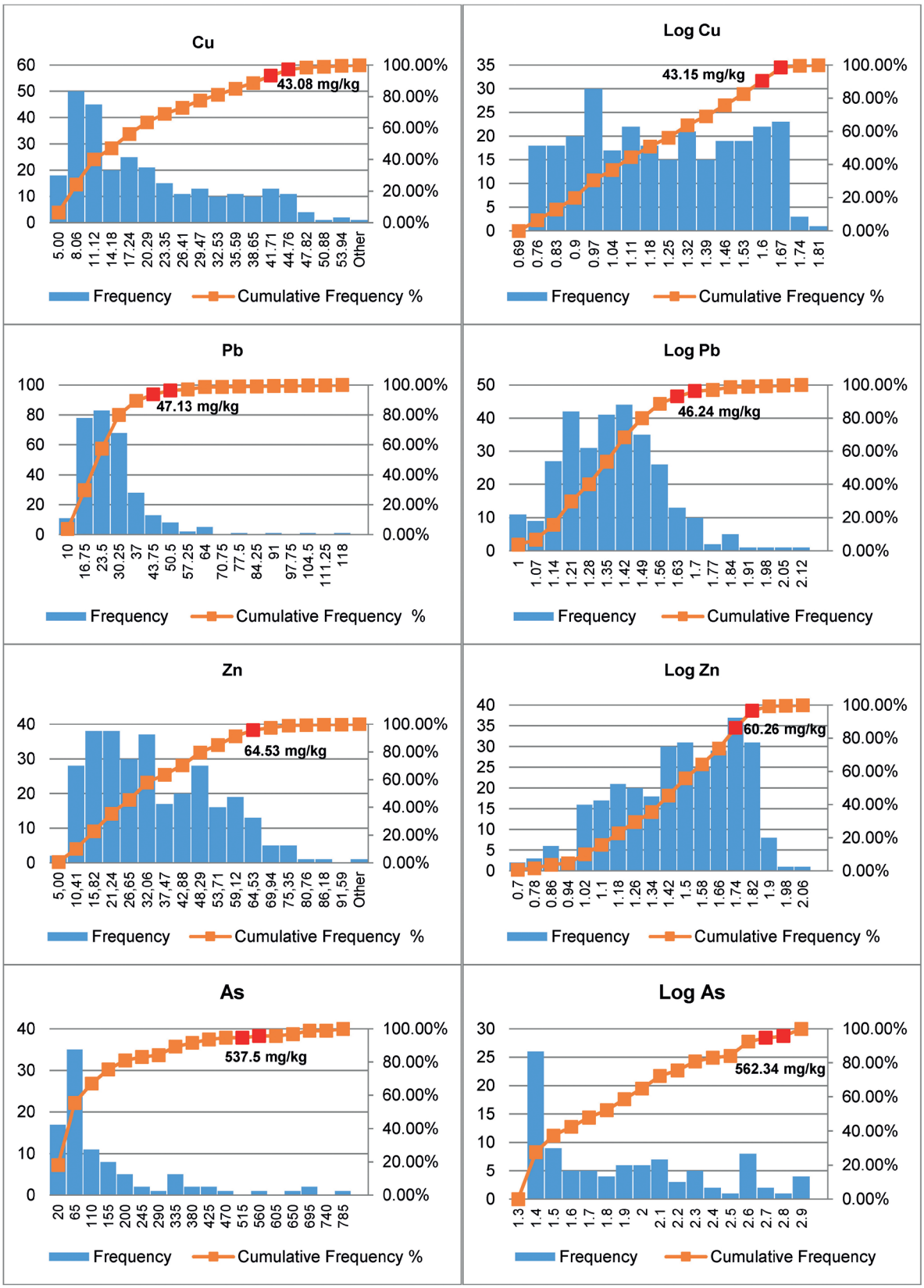

Figure 2. Class ranges frequency and cumulative frequency of the elements examined in the area.

Figure 2. ... Continued

Table 3. Descriptive statistics of the Kısacık gold enrichment area, and the threshold and background values of the elements.

	Cu mg/kg	Pb mg/kg	Zn mg/kg	As mg/kg	Mo mg/kg	Sb mg/kg	Ag mg/kg	Au mg/kg
N	281	300	299	94	179	23	17	136
Minimum	5.00	10.00	5.00	20.00	5.00	10.00	5.00	40.00
Maximum	57.00	118.00	97.00	780.00	2950.00	54.00	40.00	8200.00
Mean	18.97	24.42	31.93	129.36	218.01	19.70	8.71	350.66
Median	15.00	21.50	29.00	56.00	165.00	15.00	7.00	125.00
Std. Deviation	12.53	13.37	18.16	166.09	272.04	11.86	8.25	782.28
Kurtosis	-0.48	12.57	-0.36	4.24	57.50	3.50	15.20	75.90
Skewness	0.81	2.75	0.59	2.12	6.24	1.90	3.82	7.83
Geo. Mean	15.16	21.89	26.53	68.17	139.91	17.29	7.27	155.98
NDGT[1]	43.08	47.13	64.53	537.5	603.15[$]	51.25	9.67[$]	1189.85[$]
LDGT[2]	43.15	46.24	60.26	562.34	537.13[$]	50.12	9.33[$]	1145.51[$]
M+2*MAD	31	34.5	57	128	359	25	11	275
C-A Threshold[3]	16; 20; 40	21,97; 47,97; 63,39	21,98; 45,92; 57,94	20; 100; 329; 650	5; 60; 185; 1000	10; 20; 31;50	5; 7; 10	40; 300; 900; 1650; 2100
Background[4]	28	17	67	4.8	1.1	0.4	0.053	5

[1]Threshold from normal distribution graphic (NDGT), [2]Threshold from Lognormal distribution graphic (LDGT), [3]Threshold from C-A graphic, [4]Rudnick and Gao 2010, [$]:threshold value calculated by omitting extreme values, [*]accepted value for threshold).

Table 4. Kolmogorov-Smirnov and Shapiro-Wilk normality tests of raw and logarithmic transformed data.

	Kolmogorov-Smirnov[a]			Shapiro-Wilk		
	Statistic	df	Sig.	Statistic	df	Sig.
Cu	0.156	281	0.000	0.890	281	0.000
Pb	0.144	300	0.000	0.780	300	0.000
Zn	0.094	299	0.000	0.950	299	0.000
As	0.255	94	0.000	0.690	94	0.000
Mo	0.217	179	0.000	0.546	179	0.000
Sb	0.207	23	0.012	0.763	23	0.000
Ag	0.379	17	0.000	0.444	17	0.000
Au	0.346	136	0.000	0.358	136	0.000
LogCu	0.095	281	0.000	0.950	281	0.000
LogPb	0.056	300	0.024	0.976	300	0.000
LogZn	0.083	299	0.000	0.967	299	0.000
LogAs	0.145	94	0.000	0.902	94	0.000
LogMo	0.069	179	0.038	0.978	179	0.007
LogSb	0.144	23	0.200[*]	0.903	23	0.029
LogAg	0.229	17	0.018	0.700	17	0.000
LogAu	0.128	136	0.000	0.920	136	0.000

*. This is a lower bound of the true significance; a. Lilliefors Significance Correction.

Table 5. Spearman correlation coefficients between examined elements.

Spearman's rho	Cu	Pb	Zn	As	Mo	Sb	Ag	Au
Cu	1.00							
Pb	-0.31**	1.00						
Zn	0.75**	-0.23**	1.00					
As	-0.40**	0.67**	-0.30"	1.00				
Mo	-0.28**	0.28	-0.19	1.00**	1.00			
Sb	-0.03	0.56**	0.08	0.54*	0.37	1.00		
Ag	0.14	0.16	-0.155	c	-0.11	0.02	1.00	
Au	-0.18	0.16	-0.23**	0.08	0.13	0.51	0.11	1.00

**Correlation is significant at 0.01 level (2-tailed).
*Correlation is significant at 0.05 level (2-tailed)
cCannot be computed because at least one of the variables is constant

transformed data, in 281 points of the total 305 sampling points, the detected Cu concentrations were over the detection limits. On examination of the frequency/percentage graph for Cu, threshold values were defined as 43.08 mg/kg and 43.15 mg/kg for NDGT and LDGT respectively (Figure 2, Table 3). According to the MMAD, the threshold value for Cu was found to be 31 mg/kg (Table 3). According to the C-N method, 3 different threshold values were found for Cu: 16, 20, and 40 mg/kg (Table 3, Figure 3).

The concentration is between 10 and 118 mg/kg for 300/305 samples of Pb (Table 3, Figure 2). Considering the frequency-percent cumulative distribution graphs (for both raw data and logarithmically transformed data) for Pb, the threshold value was determined as 47.13 for the raw data (NDGT) and 46.24 mg/kg for the logarithmic transformed data (LDGT). Both threshold values are close to each other, about three times the background value (17 mg/kg). The threshold value obtained according to MMAD is 34.5 mg/kg, slightly higher than twice the background value (Table 3). Three different threshold values were determined for Pb according to the C-N multifractal method, 21.97 mg/kg, 47.97 mg/kg and 63.39 mg/kg (Table 3, Figure 3). The fact that the threshold values obtained are several times higher than the background value indicates Pb enrichment in the soil compared to the rock.

On analysis of the frequency/percentage distribution graph for 299/305 samples of Zn, for raw data and logarithmically transformed data, threshold values were defined as 64.53 mg/kg and 60.26 mg/kg respectively (Figure 2, Table 3). According to the MMAD, the threshold value for Zn was found to be 57 mg/kg (Table 3). Considering the C-N method, three different threshold values were determined for Zn: 21.98, 45.92 and 57.94 mg/kg (Figure 3, Table 3).

For the arsenic (As), analysis of the frequency/percentage distribution graph plotted for 94 samples shows that there is a concentration between 20 and 780 mg/kg, and that there is a wide range between 20 and 780 mg/kg. This range becomes more significant on consideration of the fact that the value of abundance in the upper crust is 4.8 mg/kg. High As values in the field also show that there is an intense hydrothermal alteration. Since both the raw data and logarithmic transformed data histograms of arsenic (As) were excessively skewed to the right, the threshold values obtained by conventional methods were much higher than expected. NDGT: 537.5 mg/kg, LDGT:562.34 mg/kg, MMAD (M+2*MAD): 128 mg/kg (Table 3, Figure 2). Since the detection limit of arsenic (As) is high as a disadvantage of the method used in elemental analysis in this study, the direct detection limit was accepted as the threshold value (20 mg/kg). Due to the restrictive effect of the high detection limit, the lowest threshold value was calculated as 20 mg/kg according to the C-N multifractal method. According to this method, the other three threshold values were determined as 100 mg/kg, 329 mg/kg, and 650 mg/kg, respectively (Table 3, Figure 3).

The Mo was detected at 223 points, above the detection limit. On examination of the frequency/percentage distribution graph is examined, the Mo values are concentrated between 2 and 1050 mg/kg, with a max value of 2950 mg/kg. The concentrations are distributed over a fairly wide range. According to the frequency-percent cumulative distribution graphs, the threshold value for raw data was found to be 603.15 mg/kg and for logarithmically converted data 537.13 mg/kg (Table 3, Figure 2). The threshold value found according to the MMAD method is 359 mg/kg (Table 3). Since the intense hydrothermal alteration in the region causes high Mo enrichment in the soil. So, the local threshold value was

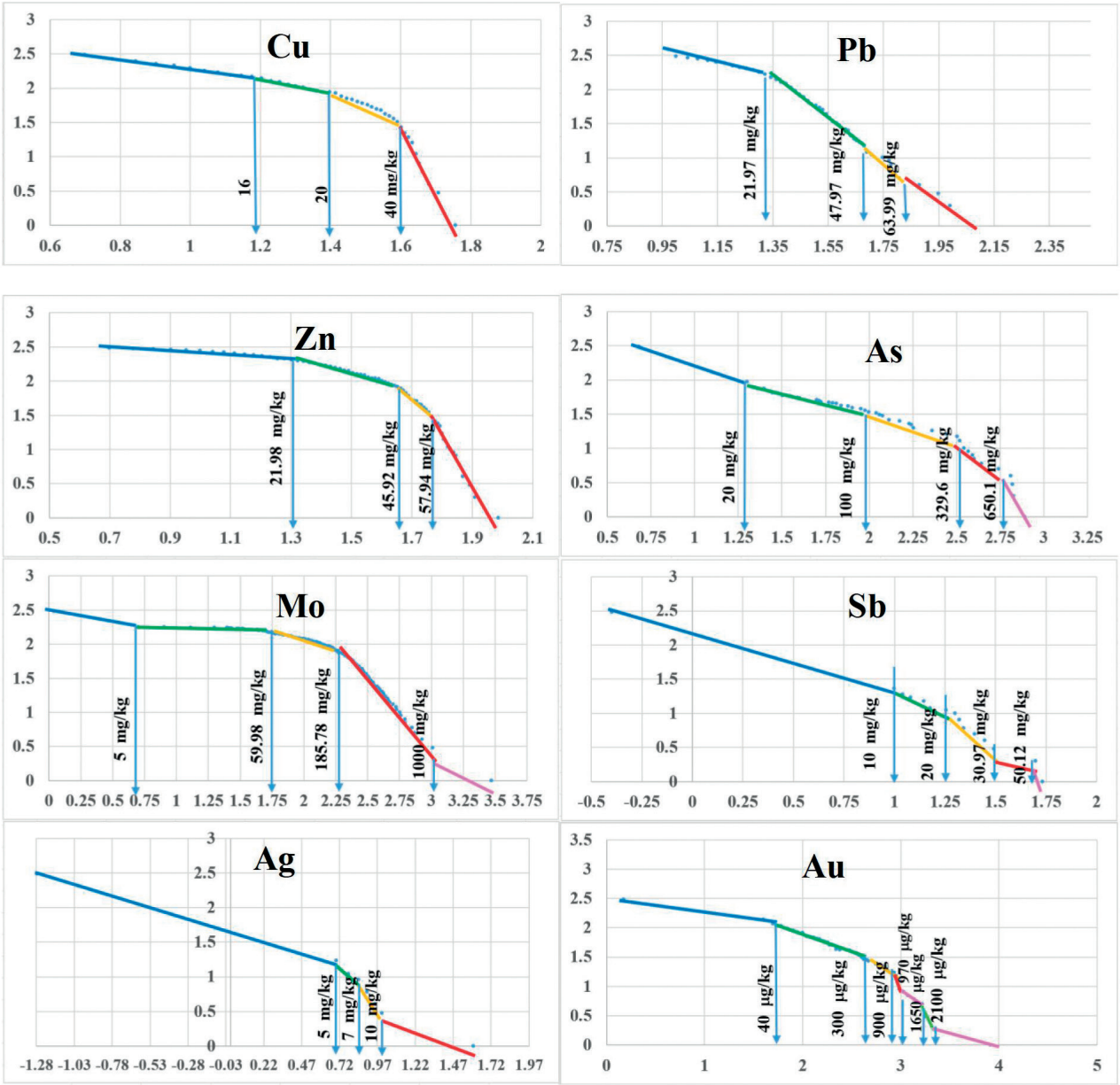

Figure 3. C-N Log-log plots for elements Cu, Pb, Zn, As, Mo, Sb, Ag and Au.

found to be quite high compared to the regional threshold values (Atkinson, 1967; Rudnick and Gao, 2010; Sun et al., 2010; Daya, 2015; Reimann et al., 2018; Lin et al., 2019)we test the small molecule flexible ligand docking program Glide on a set of 19 non-α-helical peptides and systematically improve pose prediction accuracy bynhancing Glide sampling for flexible polypeptides. In addition, scoring of the poses was improved by post-processing with physics-based implicit solvent MM-GBSA calculations. Using the best RMSD among the top 10 scoring poses as a metric, the success rate (RMSD ≤ 2.0 Å for the interface backbone atoms. According to the C-N multifractal method, 4 different thresholds were determined: 5 mg/kg, 60 mg/kg, 185 mg/kg and 1000 mg/kg (Table 3, Figure 3). If the Mo analysis was performed with a detection limit of less than 5 mg/kg, the smallest threshold value found according to the C-N method would be lower. However, since there is high Mo enrichment in the study area, the threshold values obtained were deemed sufficient to understand the area.

The Sb could not be observed in all locations. Values over the detection limit were observed in only 26 sampling points. On analysis of the frequency/percentage distribution graphs prepared for these sampling points, there is a concentration between 2 and 40 mg/kg. For Sb, both raw data and logarithmically transformed data did not show normal distribution. The threshold values obtained by conventional methods (NDGT, LDGT and MMAD) are 51.25 mg/kg, 50.12 mg/kg and 25 mg/kg, respectively. With the C-N method, 4 different threshold values were obtained: 10 mg/kg, 20 mg/kg, 31 mg/kg and 50 mg/kg (Table 3, Figure 3). The fact that the detection limit of Sb was quite high compared to the background value (0.4 mg/kg) caused the local threshold values to be higher than expected. However, due to the enrichment of many elements due to hydrothermal alteration and being a potential mineralization area, it has not contributed negatively to the exploration study in the area.

In the area, Ag and Au values were obtained in only 17 and 136 sampling points, respectively. Considering that the Ag background value is 0.053 mg/kg and the Au background value is 5 mg/kg, the detection limits for Ag and Au belonging to the area, which are 5 mg/kg and 40 mg/kg, respectively, are quite high. For both Ag and Au, the normal distribution could not be obtained for the raw data and logarithmically transformed data. Conventionally obtained threshold values are 9.67 mg/kg, 9.33 mg/kg and 11mg/kg (NDGT, LDGT and MMAD, respectively) for Ag and 1189.85 mg/kg, 1145.51mg/kg and 275 mg/kg (NDGT, LDGT and MMAD, respectively) for Au (Table 3, Figure 2) (When calculating the threshold values for Ag and Au, the extreme values were removed). With the C-N method, 3 threshold values (5mg/kg, 7 mg/kg and 10 mg/kg) were obtained for Ag and 5 threshold values (40 mg/kg, 300 mg/kg, 900 mg/kg and 1650mg/kg) for Au (Table 3, Figure 3).

Median plus two standard deviation values that were calculated as threshold values were higher than expected (both raw data and logarithmically transformed data) (Table 3), since the analyses were performed with high detection limits. Threshold values obtained with MMAD were found to be relatively lower, although they were affected by analyzes performed with a high detection limit. The threshold values obtained by the C-N method, on the other hand, gave more robust results despite the analysis limitation with high detection limits. Detection limits can be used as threshold values in studies to get an idea, especially in cases where the detection limits are higher than the background values.

Single element mapping

Anomaly-isoconcentiation maps were created via the ordinary Kriging predicting technique for Ag and Au, as well as for the Cu, Zn, Pb, Sb, As and Mo elements that are pathfinder elements in gold exploration, using the Arc-Map 10.50 software. The Kriging technique eases the estimations of variations in unsampled points with high precision by using structural factors obtained from semivariograms. In the technique, it is necessary to determine the most suitable spatial weights for sampling points. This method is one of the most useful methods developed for estimating the unknown values of the surrounding points by using the variations in known values (Matheron, 1963; Baczkowski and Clark, 1981; Vural and Şahin, 2012; Vural and Erdoğan, 2013, 2014). Therefore, it is preferable to the other methods. Anomaly-isoconcentration maps were thus prepared for Cu, Zn, Pb, Sb, As, Mo, Ag and Au elements in the field by applying the ordinary Kriging prediction method to the data obtained from the semivariogram model (Figure 4).

On evaluation of the anomaly map of the Kısacık field for Cu, the Cu distribution in the field is intensified in two main sites. The first site is in the south-west area of the field that includes altered, intense limonitization and hematitization and the second site is in the north-east area of the field where there is also intense limonitization and hematitization. The common property of the anomalies is that they are either on and/or near the tectonic lines. They are encountered particularly in the south and north-west of the field where there is intense hematitization and limonitization related to the faults, and in places where volcanic rocks are cut by capillary silica veins.

It is evident that the Zn distribution in the field is like the Cu distribution, in line with the correlation analysis. The Pb distribution in the field is concentrated in the area where NE-SW- orientated tectonic line and NW-SE-orientated tectonic line intersect. The Pb distribution map shows similarities with the Sb and Mo distribution maps. On analysis of the distribution maps created for As, a concentration on the tectonic lines can be seen, even though it does not overlap completely with the Cu and Zn distribution maps. High As areas increase in size in tectonic lines where there is intense hematitization and limonitization.

Even though the silver anomaly map does not completely overlap with other anomaly maps, the Ag anomaly can be seen in the south-west part of the area where two tectonic lines intersect. On analysis of the gold anomalies in the field, it is evident that the anomalies cover silver anomalies, and that they lie along tectonic lines and, in the parts, where there is hematitization and sericitization.

Figure 4 presents the halos for gold and its pathfinders in the soil above the Kısacık mineralization. These halos show that the geochemical anomalies are based on the background value of the element examined (Rudnick and

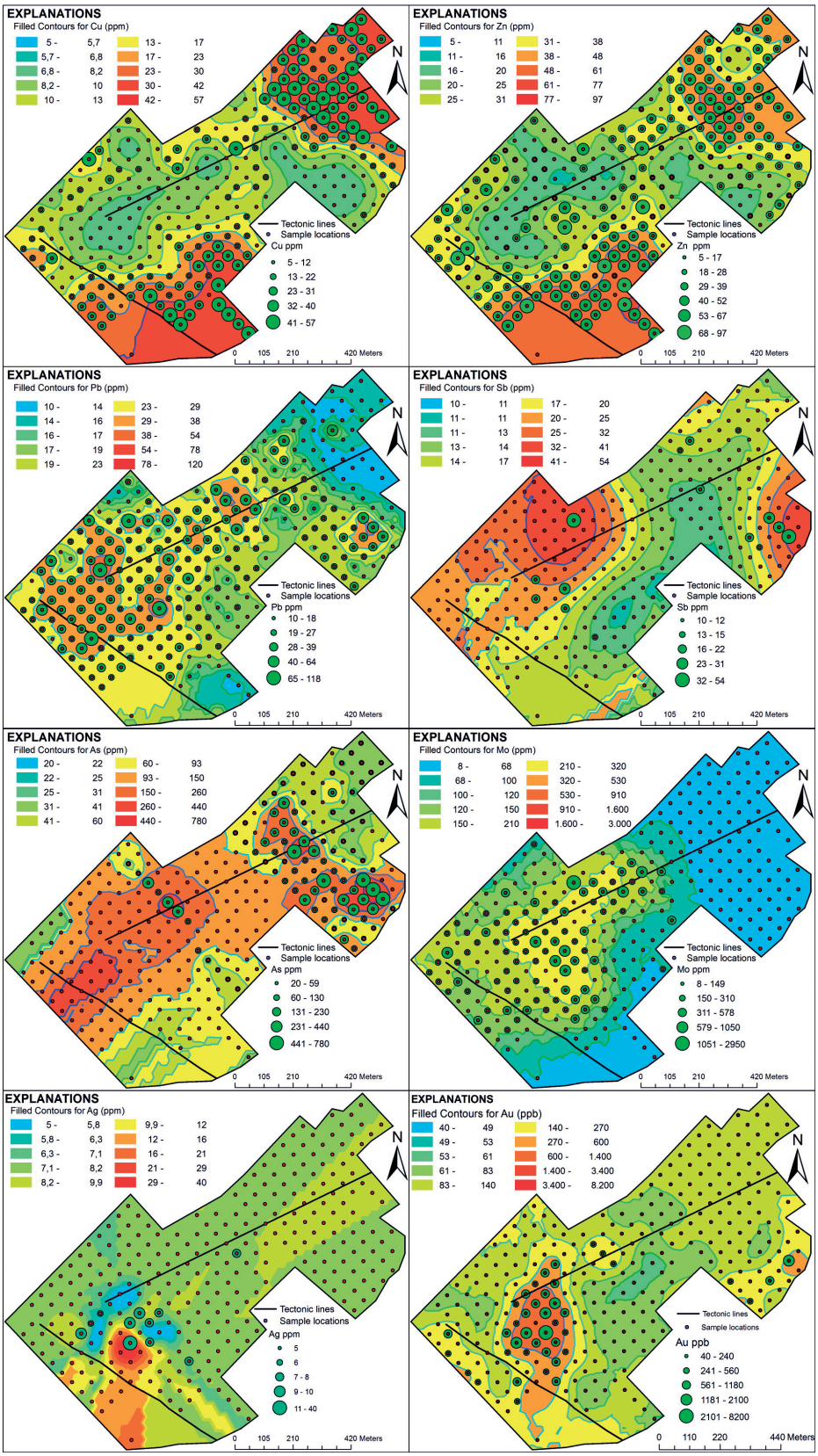

Figure 4. Anomaly-isoconcentration and dot maps of the study area for elements examined.

Gao, 2010). On analysis of the element anomaly maps of all elements, no sufficient surface enrichment can be seen in the field since the data obtained are not strong. Consequently, they characterize poorly the superficial signature produced by possible buried mineralization.

Multielement haloes technique

According to Reis et al., (2001), geochemical haloes around ore bodies can be better defined by the combination of two or more pathfinder elements. Multi-element halos are less influenced by the effects of random errors, and consequently exhibit a closer relationship to structural geological features associated with a particular mineralization. Thereby, the reliability of the interpretation of the halos is increased and vulnerable data due to high detection limits are enhanced.

In forming the element halos, the elements in the halo at each sampling point are normalized by being divided by background values for each sampling point and summed so that the multi-element value of the point being analyzed is obtained. The other part of the procedure is calculating the threshold values for the values obtained. As mentioned above, there are a number of methods for this calculation (Vural, 2014, 2015c, 2020; Vural and Aydal, 2020a; Vural and Çiçek, 2020). C-N fractal method was used here (Figure 5), C donates the multi-element value of the sampling point and N donates number of the obtained value. Calculating the data for multi-element halos can be formulized as follows:

$$H_{x+y} = \left(\frac{X_1}{X_0} + \frac{Y_1}{Y_0}\right); \ldots\ldots\ldots\ldots \left(\frac{X_N}{X_0} + \frac{Y_N}{Y_0}\right) \qquad 6)$$

where X_i, X_2, X_N are concentrations of X in samples, 1, 2,…..; N, Y_1 Y_2, ..., Y_N are concentrations of Y in samples 1, 2…N, and X_0, Y_0 are background values for X and Y data populations.

In forming the multi-element halos to be used for the enhancement of vulnerable data, three different multi-element halo maps were formed using defining statistical parameters and correlation coefficients (Cu+Zn, Sb+Pb+As+Mo and As+Ag+Au multi-element halos). The concerned multi-element values of the field were calculated and anomaly-isoconcentration maps (multi-element halo map) were formed using the ordinary Kriging predicting method (Figure 6).

From the anomaly maps formed by the multi-element halo method, it can clearly be seen that there is an improvement when they are compared to the single-element anomaly maps. According to the multi-element technique, the target area was calculated as 325.14 m^2 in the As+Ag+Au multi-element halo anomaly map, which has a first-degree importance for gold. A significant

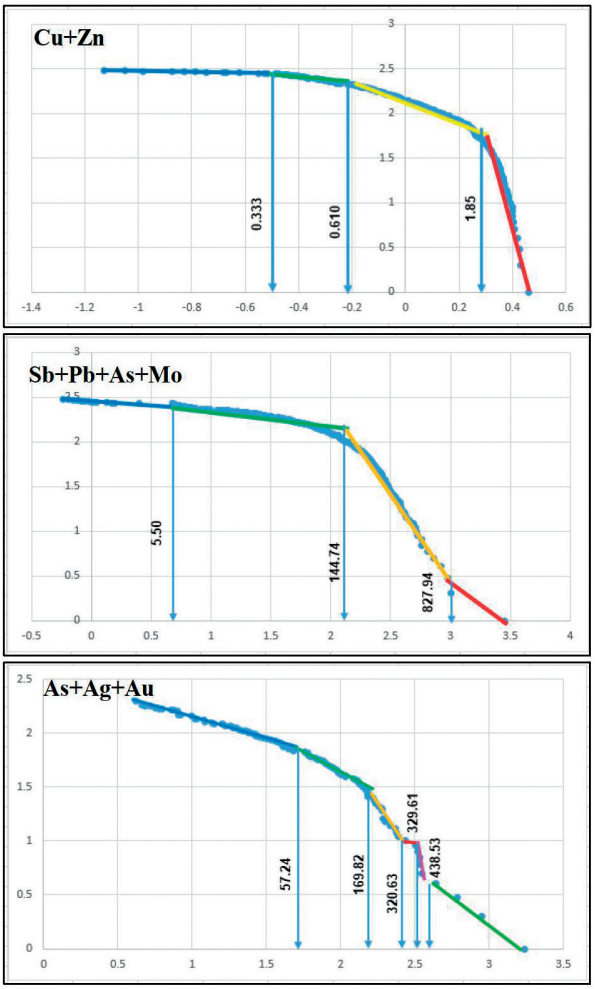

Figure 5. C-N Log-log plots for multi-elements [(Cu+Zn), (Sb+Pb+As+Mo) and (As+Ag+Au)].

improvement occurred for other sites where the multi-element halo method was employed. On analysis of the map, new target sites in the area are clearly evident which were not apparent in single-element maps. There is also a visible improvement for Cu+Zn halo anomaly maps when compared with their individual single anomaly maps. However, this multi-element halo map of Cu+Zn is not compliant with other multi-element anomaly maps, due to the lack of strong correlation coefficients between them (Table 5).

Several exploration drills have been made in the study field by MTA. Drill locations were selected as places where there are anomalies for gold, and parts where there is intense haematitization, limonitization and sericitization as well as an abundance of capillary silica veins. On analysis of the drill data of areas in which potential is seen in the multi-element halo anomaly maps

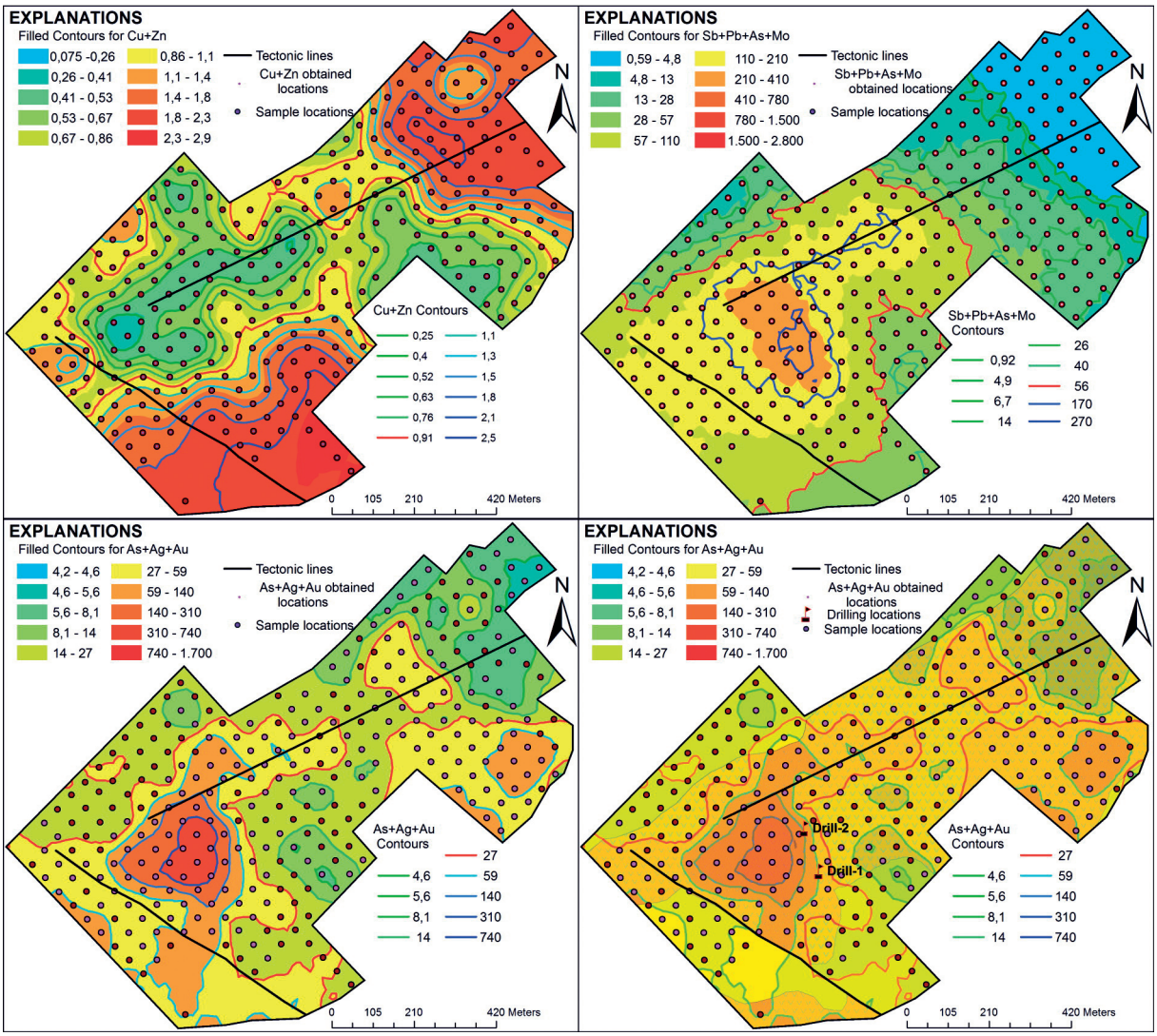

Figure 6. Multi-element halo-anomaly maps of the Kısacık gold enrichment area (the red line is the threshold for the multi-element halos, a) Cu+Zn multi-element halo anomaly map. b) Sb-Pb-As-Mo multi-element halo anomaly map. c) As+Ag+Au multi-element halo anomaly map. d) As+Ag+Au multi-element halo anomaly map. embedded in the geology of the area with drilling locations (a detailed explanation of the geology of the area is given in Figure 1).

formed within the scope of this study, clear and positive correlations among Sb, As, Ag and Au values obtained from drill 1 are evident (Figure 7). The significant values for gold can be seen in the initial 100 meters of the drills. Generally, a clear positive correlation between gold enrichment and the element As is seen in drilling-core assessments. Similar correlation values occur between Au and Sb, Mo and Ag. This positive-correlation relationship in the drill data shows conformity with soil geochemistry values in the field.

The first gold enrichment in drill 1 is within the initial 10-25 m. At this depth, volcanic rocks are available and an intense silicification can be observed. Moreover, chalcedonic quartz bands are observed, and the breccia rock texture is dominant. Limonite fillings and pyritization are encountered in the cracks. At the depths where the second most important gold enrichment occurred in drill 1, altered lithic tuffs are available. Manganese filling is significant in the cracks. Sericitization is highly evident and dispersed pyrites are encountered. In particular, iron oxide and manganese veinlets are characteristic in this area. Capillary silica veins usually bear a close relationship to mineralization. Similar lithology and mineral groups are observed in the parts where the third most important gold enrichment occurred. Chloritization and kaolinitization are seen in volcanic rock with an

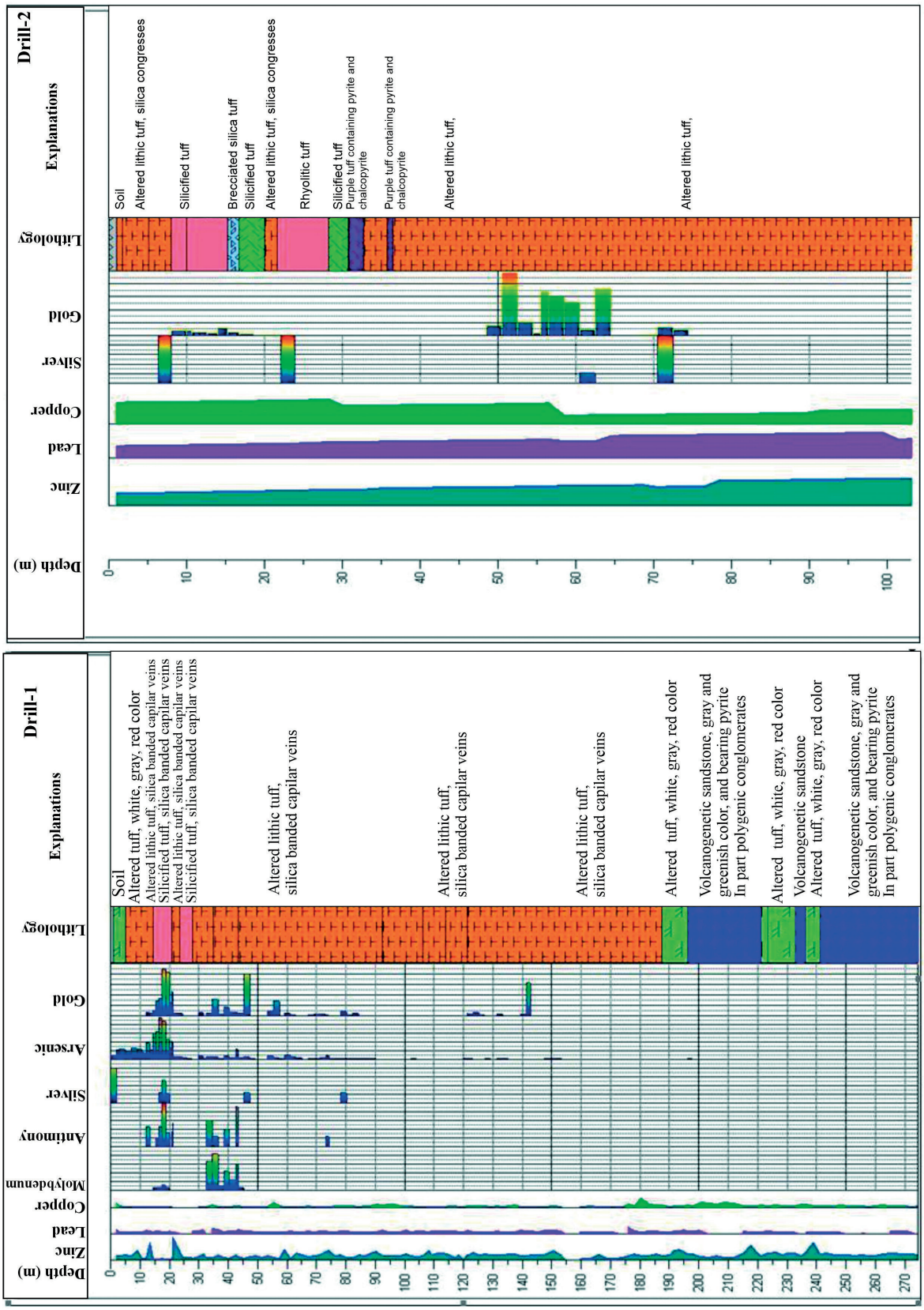

Figure 7. Drill log data of the area (After Vural, 2006).

agglomerated appearance. Sericitization is encountered in this area, as in the others (Figure 7).

On analysis of the drill 2 of MTA, it is evident that gold enrichment occurred in the initial 100 m. Kaolinitization, chloritization, the creation of limonite and hematite bands, cemented manganese and capillary silica veinlets accompany gold enrichment in this drill (Figure 7).

DISCUSSION

Soil geochemistry studies are an important integral part of the exploration for natural resources, although they are not the whole process. In the exploration process, many studies such as general geology, structural geology, mineralogy, alteration geochemistry, geophysics and drilling are carried out in coordination with each other (Macheyei et al., 2020). In the soil geochemistry study, which has an important place among these methods, it is especially important to evaluate the data in the most appropriate/correct way (Agterberg, 2012; Afzal et al., 2015). Determining the threshold values of the elements in the soil and determining the element mobility characters and distribution patterns and plotting element distribution maps is an important step in the evaluation of soil geochemistry data (Divrikli et al., 2006; Karada et al., 2006; Carranza, 2009b; Sungur et al., 2014, 2015, 2016, 2020; Macheyei et al., 2020). New methods are always suggested, especially in estimating the threshold values of the elements in the soil (Arik and Yaldiz, 2010; Meigoony et al., 2014; Zuo and Wang, 2015; Zuo et al., 2015; Wang et al., 2017; Xiong et al., 2018; Ahmadfaraj et al., 2019; Macheyei et al., 2020).

The author carried out studies for orientation purposes and made comparisons with some of these studies with his own data. It has been seen in these studies that the methods have advantages over each other in different fields. As a disadvantage of the analysis method used in this study, since the detection limits of As, Mo, Sb, Ag and Au elements are high, concentrations of these elements could not be obtained at each sampling point. Therefore, difficulties arose in calculating the threshold values of the elements. C-N Fractal method gave the most satisfactory results in the threshold value calculations. In the second place, satisfactory threshold values were obtained by the MMAD method. Again, as a result of performing analyzes with a high detection limit, considering that satisfactory results cannot be obtained in single element distribution maps, multielement distribution maps were plotted with the pathfinder elements associated with gold and silver using the multielement halos technique. Multi element halos element distribution maps gave very satisfactory results for the field. It was observed that the drilling data made in the field confirmed the findings obtained with this technique. Since the field was modeled in 3D with the drilling data, it can be said that other sophisticated data evaluation methods, such as fractal/multi fractal models, C-A, C-D, S-V etc. (Cheng et al., 1994; Li et al., 2003; Carranza et al., 2009; Carranza and Sadeghi, 2010; Afzal et al., 2012; Wang et al., 2013; Xiong et al., 2018), can be used in the field for comparison purposes.

CONCLUSIONS

In this study, soil geochemistry survey was carried out for gold exploration at the Kısacık area (Ayvacık, Çanakkale/Türkiye) using iso-concentration mapping for single element and multi-element halos techniques. The threshold values of the elements were calculated with different approaches and compared with each other. As a result of the comparison, it was seen that the threshold values calculated by the MMAD method gave acceptable results, but it was seen that the C-N fractal method gave much more realistic (robust) threshold values. With the MMAD method, the threshold values of Cu, Pb, Zn, As, Mo, Sb, Ag and Au elements were calculated as (Au in mg/kg, other elements in mg/kg) 31, 34.5, 57, 128, 359, 25, 11 and 275, respectively. Due to the logic of the C-N fractal method, multiple threshold values can be calculated for the elements depending on the geochemical properties of the area. So, the minimum threshold values calculated for Cu, Pb, Zn, As, Mo, Sb, Ag and Au elements by C-N method (Au mg/kg, other elements in mg/kg) are 16, 21.97, 21.98, 20, 5, 10, 5, and 40, respectively. Since, As, Mo, Sb, Ag, and Au analysis of samples taken from the field are performed at high detection limits, detection limits are also accepted as threshold values for these elements, which are also consistent with the C-N minimum threshold results.

By using Cu, Zn, Pb, As, Sb, Mo, Ag and Au concentrations in Kısacık soil samples, different methods were also applied to improve the representation of the superficial geochemical signature. For this purpose (within the scope of soil geochemistry study-exploration geochemistry study) for gold in the area, single element anomaly maps of elements and multi-element halos anomaly maps were plotted. The maps obtained by the two methods were compared, and their functionality was also checked by drilling in the area. It has been demonstrated that multi-element halo anomaly maps yield significantly more satisfactory results than single-element iso-concentration anomaly maps.

Cu+Zn anomalies by the multi-element halo technique shows enrichment towards the edges of the center in the north-east and south-west. This can be explained by the relatively mobile character of the Cu and Zn elements. Combining As, Ag, and Au widens the anomaly area, enhancing gold exploration potential. Though ineffective individually, As, Sb, Mo, and Pb become valuable through

the multi-element halo technique.

Consequently, C-N fractal methods effectively determined element thresholds for geochemical prospecting. The multi-element halo technique further enhanced weak anomaly assessment. Drilling confirmed these findings, demonstrating the efficacy of soil geochemistry with C-N fractal multi-element halo analysis for locating buried mineral deposits.

ACKNOWLEDGEMENTS

The author dedicates this study to the Department of Geological Engineering (Ankara Geology) on the occasion of its 90th anniversary in education (1934-2024). This study is supported by the General Directorate of Mineral Research and Exploration (MTA, Ankara) during the author's Ph.D. studies. The author gives thanks to all of MTA's officials and to his supervisor Prof.Dr. Doğan Aydal (Ankara University) for the contributions during the author's doctoral studies. A special thanks to Ali Gündoğdu for his contributions to the analytical processes.

Declarations

- *Funding*: No fundings.
- *Conflicts of interest/Competing interests:* The author declares that he has no competing interests.
- *Availability of data and material:* Data supporting Figure 2-6, Tables 3-5 are available on request from the corresponding author.
- *Authors' contributions:* The entire article, the figures and tables used were produced by the corresponding author, Alaaddin Vural. The data used in the article is the data of the author's doctoral work and has been evaluated with a new perspective by the author.

This article does not contain any studies with human participants or animals performed by the author, so:

- *Ethics approval:* Not applicable
- *Consent to participate:* Not applicable
- *Consent for publication:* Not applicable.

REFERENCES

Afzal P., Alghalandis Y.F., Moarefvand P., Omran N.R., Haroni H.A., 2012. Application of power-spectrum-volume fractal method for detecting hypogene, supergene enrichment, leached and barren zones in Kahang Cu porphyry deposit, Central Iran. Journal of Geochemical Exploration 112, 131-138. doi: 10.1016/j.gexplo.2011.08.002.

Afzal P., Ghasempour R., Mokhtari A.R., Haroni H.A., 2015. Application of Concentration-Number and Concentration-Volume Fractal Models to Recognize Mineralized Zones in North Anomaly Iron Ore Deposit, Central Iran. Archives of Mining Sciences 60, 777-789. doi: 10.1515/amsc-2015-0051.

Afzal P., Tehrani M.E., Ghaderi M., Hosseini M.R., 2016. Delineation of supergene enrichment, hypogene and oxidation zones utilizing staged factor analysis and fractal modeling in Takht-e-Gonbad porphyry deposit, SE Iran. Journal of Geochemical Exploration 161, 119-127. doi: 10.1016/j.gexplo.2015.12.001.

Agterberg F.P., 2012. Multifractals and geostatistics. Journal of Geochemical Exploration 122, 113-122. doi: 10.1016/j.gexplo.2012.04.001.

Ahmadfaraj M., Mirmohammadi M., Afzal P., Yasrebi A.B., Carranza E.J., 2019. Fractal modeling and fry analysis of the relationship between structures and Cu mineralization in Saveh region, Central Iran. Ore Geology Reviews 107, 172-185. doi: 10.1016/j.oregeorev.2019.01.026.

Aitchison J., 1986. The Statistical Analysis of Compositional Data. Chapman and Hall, London.

Alfaro M.R., Nascimento C.W.A. do, Biondi C.M., Silva Ygor Jacques Agra Bezerra da Silva, Yuri Jacques Agra Bezerra da Accioly, A.M. de A., Montero A., Ugarte O.M., Estevez J., 2018. Rare-earth-element geochemistry in soils developed in different geological settings of Cuba. Catena 162, 317-324. doi: 10.1016/j.catena.2017.10.031.

Altunkaynak Ş. and Genç Ş.C., 2008. Petrogenesis and time-progressive evolution of the Cenozoic continental volcanism in the Biga Peninsula, NW Anatolia (Turkey). Lithos 102, 316-340. doi: 10.1016/j.lithos.2007.06.003.

Anand R.R., Hough R.M., Salama W., Aspandiar M.F., Butt C.R.M., González-Álvarez I., Metelka V., 2019. Gold and pathfinder elements in ferricrete gold deposits of the Yilgarn Craton of Western Australia: A review with new concepts. Ore Geology Reviews 104, 294-355. doi: 10.1016/j.oregeorev.2018.11.003.

Arik F. and Yaldiz T., 2010. Heavy metal determination and pollution of the soil and plants of southeast Tavşanli (Kütahya, Turkey). Clean - Soil, Air, Water 38, 1017-1030. doi: 10.1002/clen.201000131.

Atkinson W.J., 1967. Regional Geochemical Studies in County Limerick, Ireland, with Particular Reference to Selenium and Molybdenum. University of London.

Ayad A., 2023. Mapping of potential groundwater recharge sites in the Smaâla area (Central Morocco). Journal of African Earth Sciences 200, 104888. doi: 10.1016/j.jafrearsci.2023.104888.

Ayad A. and Bakkali S., 2022. Multifractal Classification of the Disturbed Areas of the Sidi Chennane Phosphate Deposit, Morocco. Economic and Environmental Geology 55, 231-239. doi: 10.9719/EEG.2022.55.3.231.

Aydal D., Vural A., Taşdelen Uslu İ., Aydal E.G., 2007. Crosta Technique Application on Bayramiç (Alakeçi-Kısacık) Mineralized Area by Using Landsat 7 Etm+ Data. Journal of Engineering and Architecture Faculty of Selcuk University 22, 29-40.

Aydal D., Vural A., Taşdelen Uslu İ., Aydal E.G., 2006a. Investigation of Kuşçayırı-Kartaldağı (Bayramiç-Çanakkale) mineral enhancement region by Crosta technique with LANDSAT 7 ETM+ bands. Technical University of İstanbul,

First Remote Sensing Workshop and Panel. İstanbul, Türkiye, 11.

Aydal D., Vural A., Taşdelen Uslu İ., Aydal E.G., 2006b. Crosta Technique Application on Bayramic (Alakeçi-Kisacik) Mineralized Area by Using Landsat 7 TM Data. 30th Anniversary Fikret Kurtman Geology Symposium. Konya, Türkiye, 195.

Baczkowski A.J., Clark I., 1981. Practical Geostatistics. Journal of the Royal Statistical Society. Series A (General) 144, 537. doi: 10.2307/2981833.

Bech J., Tume P., Sokolovska M., Reverter F., Sanchez P., Longan L., Bech J., Puente A., Oliver T., 2008. Pedogeochemical mapping of Cr, Ni, and Cu in soils of the Barcelona Province (Catalonia, Spain): Relationships with soil physico-chemical characteristics. Journal of Geochemical Exploration 96, 106-116. doi: 10.1016/j.gexplo.2007.03.005.

Bingöl E., 1975. Geology of Biga Peninsula and some characteristics of Karakaya Formation. International Geodynamics Project, Report of Turkey. Maden Tetkik ve Arama Genel Müdürlüğü, Ankara, Turkey, 71-77.

Bounessah M. and Atkin B.P., 2003. An application of exploratory data analysis (EDA) as a robust non-parametric technique for geochemical mapping in a semi-arid climate. Applied Geochemistry 18, 1185-1195. doi: 10.1016/S0883-2927(02)00247-0.

Carranza E.J.M., 2017. Natural Resources Research Publications on Geochemical Anomaly and Mineral Potential Mapping, and Introduction to the Special Issue of Papers in These Fields. Natural Resources Research 26, 379-410. doi: 10.1007/s11053-017-9348-1.

Carranza E.J.M., 2009a. Geochemical Anomaly and Mineral Prospectivity Mapping in GIS. Elsevier.

Carranza E.J.M., 2009b. Controls on mineral deposit occurrence inferred from analysis of their spatial pattern and spatial association with geological features. Ore Geology Reviews 35, 383-400. 10.1016/j.oregeorev.2009.01.001.

Carranza E.J.M. and Hale M., 2001. Logistic regression for geologically constrained mapping of gold potential, Baguio district, Philippines. Exploration and Mining Geology 10, 165-175. doi: 10.1016/S0169-1368(02)00111-7.

Carranza E.J.M., Owusu E.A., Hale M., 2009. Mapping of prospectivity and estimation of number of undiscovered prospects for lode gold, southwestern Ashanti Belt, Ghana. Mineralium Deposita 44, 915-938. doi: 10.1007/s00126-009-0250-6.

Carranza E.J.M. and Sadeghi M., 2010. Predictive mapping of prospectivity and quantitative estimation of undiscovered VMS deposits in Skellefte district (Sweden). Ore Geology Reviews 38, 219-241. doi: 10.1016/j.oregeorev.2010.02.003.

Chen D., Wei J., Wang W., Shi W., Li H., Zhan X., 2019. Comparison of Methods for Determining the Thresholds of Geochemical Anomalies and the Prospecting Direction-A Case of Gold Deposits in the Gouli Exploration Area, Qinghai Province. Minerals 9, 368. doi: 10.3390/min9060368.

Cheng Q., Agterberg F.P., Ballantyne S.B., 1994. The separation of geochemical anomalies from background by fractal methods. Journal of Geochemical Exploration 51, 109-130. doi: 10.1016/0375-6742(94)90013-2.

Darwish M.A.G. and Poellmann H., 2010. Geochemical exploration for gold in the Nile Valley Block (A) area, Wadi Allaqi, South Egypt. Chemie Der Erde - Geochemistry 70, 353-362. doi: 10.1016/j.chemer.2009.12.002.

Daya A.A., 2015. Comparative study of C-A, C-P, and N-S fractal methods for separating geochemical anomalies from background: A case study of Kamoshgaran region, northwest of Iran. Journal of Geochemical Exploration 150, 52-63. doi: 10.1016/j.gexplo.2014.12.015.

Divrikli U., Horzum N., Soylak M., Elci L., 2006. Trace heavy metal contents of some spices and herbal plants from western Anatolia, Turkey. International Journal of Food Science and Technology 41, 712-716. doi: 10.1111/j.1365-2621.2005.01140.x.

Dönmez M., Akçay A.E., Genç S.C., Acar S., 2005. Middle-Upper Eocene volcanism and marine ignimbrites in Biga Peninsula. Bulletin of the Mineral Research and Exploration 131, 49-61.

Drewnik M., Skiba M., Szymański W., Zyła M., 2014. Mineral composition vs. soil forming processes in loess soils - A case study from Kraków (Southern Poland). Catena 119, 166-173. doi: 10.1016/j.catena.2014.02.012.

Duru M., Van P., Pehlivan S., Sentürk Y., Yavas F., Kar H., 2004. New results on the lithpstratigraphy of the Kazdag Massif in northwest Turkey. Turkish Journal of Earth Sciences 13, 177-186.

Esmaeili A., Moore F., Keshavarzi B., Jaafarzadeh N., Kermani M., 2014. A geochemical survey of heavy metals in agricultural and background soils of the Isfahan industrial zone, Iran. Catena 121, 88-98. doi: 10.1016/j.catena.2014.05.003.

Filzmoser P. and Hron K., 2008. Outlier detection for compositional data using robust methods. Mathematical Geosciences 40, 233-248. doi: 10.1007/s11004-007-9141-5.

Genç Ş.C., 1998. Evolution of the Bayramiç magmatic complex, Northwestern Anatolia. Journal of Volcanology and Geothermal Research 85, 233-249.

Gerla P.J., Sharif M.U., Korom S.F., 2011. Geochemical processes controlling the spatial distribution of selenium in soil and water, west central South Dakota, USA. Environmental Earth Sciences 62, 1551-1560. doi: 10.1007/s12665-010-0641-0.

Ghezelbash R., Maghsoudi A., Carranza E.J.M., 2019. An Improved Data-Driven Multiple Criteria Decision-Making Procedure for Spatial Modeling of Mineral Prospectivity: Adaption of Prediction-Area Plot and Logistic Functions. Natural Resources Research 28, 1299-1316. doi: 10.1007/s11053-018-9448-6.

Hampel F.R., 1974. The Influence Curve and its Role in Robust

Estimation. Journal of the American Statistical Association 69, 383-393. doi: 10.1080/01621459.1974.10482962.

Hassanpour S. and Afzal P., 2013. Application of concentration-number (C-N) multifractal modeling for geochemical anomaly separation in Haftcheshmeh porphyry system, NW Iran. Arabian Journal of Geosciences 6, 957-970. doi: 10.1007/s12517-011-0396-2.

Karacık Z. and Yılmaz Y., 1998. Geology of the ignimbrites and the associated volcano-plutonic complex of the Ezine area, Northwestern Anatolia. Journal of Volcanology and Geothermal Research 85, 251-264.

Karada M.M., Arik F., Öztürk A., 2006. Çatmakaya (Seydişehir-Türkiye) boksit yatağının kökenine jeoistatistiksel ve jeokimyasal bir yaklaşım. Distribution 27, 63-85.

Li C., Ma T., Shi J., 2003. Application of a fractal method relating concentrations and distances for separation of geochemical anomalies from background. Journal of Geochemical Exploration 77, 167-175. doi: 10.1016/S0375-6742(02)00276-5.

Lin X., Wang X., Zhou J., Chi Q., Nie L., Zhang B., Xu S., Zhao S., Liu H., Sun B., Han Z., Liu D., Wang W., Liu Q., Bai J., Fan H., Ma N., Zhang L., Xu G., Wei W., Zhao B., Shen W., 2019. Concentrations, variations and distribution of molybdenum (Mo) in catchment outlet sediments of China: Conclusions from the China geochemical baselines project. Applied Geochemistry 103, 50-58. doi: 10.1016/j.apgeochem.2019.02.013.

Machender G., Dhakate R., Rao S.T.M., Rao B.M., Prasanna L., 2014. Heavy metal contamination in sediments of Balanagar industrial area, Hyderabad, Andra Pradesh, India. Arabian Journal of Geosciences 7, 513-525. doi: 10.1007/s12517-012-0759-3.

Macheyei A.., Li X., Kafumu D.P., Yuan F., 2020. Applied Geochemistry Advances in Mineral Exploration Techniques. Elsevier B.V., Amsterdam.

Mandelbrot B.B., 1983. The Fractal Geometry of Nature (Updated and Augmented Edition). W.H. Freeman, San Francisco, CA.

Matheron G., 1963. Principles of geostatistics. Economic Geology 58, 1246-1266. doi: 10.2113/gsecongeo.58.8.1246.

Mazzucchelli R.H., 1996. The application of soil geochemistry to gold exploration in the black Flag Area, Yilgarn Block, Western Australia. Journal of Geochemical Exploration 57, 175-185. doi: 10.1016/S0375-6742(96)00033-7.

Meigoony M.S., Afzal P., Gholinejad M., Yasrebi A.B., Sadeghi B., 2014. Delineation of geochemical anomalies using factor analysis and multifractal modeling based on stream sediments data in Sarajeh 1:100,000 sheet, Central Iran. Arabian Journal of Geosciences 7, 5333-5343.doi: 10.1007/s12517-013-1074-3.

Nazarpour A., Omran N.R., Paydar G.R., Sadeghi B., Matroud F., Nejad A.M., 2015. Application of classical statistics, logratio transformation and multifractal approaches to delineate geochemical anomalies in the Zarshuran gold district, NW Iran. Chemie Der Erde 75, 117-132. doi: 10.1016/j.chemer.2014.11.002.

Nichol I., Closs L., Lavin O., 1989. Sample representativity with reference to gold exploration. In: Thornton, I., Howarth, R. (Eds.), Applied Geochemistry in the 1980s. Graham and Trotman, London, 60-85.

Okay A.İ. and Altiner D., 2004. Uppermost Triassic limestone in the Karakaya Complex; stratigraphic and tectonic significance; Commemorating Okan Tekeli. Turkish Journal of Earth Sciences 13, 187-199.

Okay A.İ. and Göncüoğlu C., 2004. The Karakaya Complex: A review of data and concepts. Turkish Journal of Earth Sciences 13, 77-95.

Okay A.İ. and Satir M., 2000. Coeval plutonism and metamorphism in a latest Oligocene metamorphic core complex in northwest Turkey. Geological Magazine 137, 495-516. doi: 10.1017/S0016756800004532.

Okay A.İ., Satır M., Maluski H., Siyako M., Monie P., Metzger R., Akyüz S., Yin A., 1996. Paleoand Neo-Tethyan events in northwestern Turkey: geologic and geochronologic constraints. In: Harrison, M. (Ed.), Tectonics of Asia. Cambridge University Press, 420-441.

Okay,A.İ., Siyako M., Bürkan K.A., 1990. Biga yarımadasının jeolojisi ve tektonik evrimi. Türkiye Petrol Jeologları Derneği Bülteni 2, 83-121.

Reimann C., Fabian K., Birke M., Filzmoser P., Demetriades A., Négrel P., Oorts K., Matschullat J., de Caritat P., Albanese S., Anderson M., Baritz R., Batista M.J., Bel-Ian A., Cicchella D., De Vivo B., De Vos W., Dinelli E., Ďuriš M., Dusza-Dobek A., Eggen O.A., Eklund M., Ernsten V., Flight D.M.A., Forrester S., Fügedi U., Gilucis A., Gosar M., Gregorauskiene V., De Groot W., Gulan A., Halamić J., Haslinger E., Hayoz P., Hoogewerff J., Hrvatovic H., Husnjak S., Jähne-Klingberg F., Janik L., Jordan G., Kaminari M., Kirby J., Klos V., Kwećko P., Kuti L., Ladenberger A., Lima A., Locutura J., Lucivjansky P., Mann A., Mackovych D., McLaughlin M., Malyuk B.I., Maquil R., Meuli R.G., Mol G., O'Connor P., Ottesen R.T., Pasnieczna A., Petersell V., Pfleiderer S., Poňavič M., Prazeres C., Radusinović S., Rauch U., Salpeteur I., Scanlon R., Schedl A., Scheib A., Schoeters I., Šefčik P., Sellersjö E., Slaninka I., Soriano-Disla J.M., Šorša A., Svrkota R., Stafilov T., Tarvainen T., Tendavilov V., Valera P., Verougstraete V., Vidojević D., Zissimos A., Zomeni Z., Sadeghi M., 2018. GEMAS: Establishing geochemical background and threshold for 53 chemical elements in European agricultural soil. Applied Geochemistry 88, 302-318. doi: 10.1016/j.apgeochem.2017.01.021.

Reimann C. and Filzmoser P., 2000. Normal and log normal data distribution in geochemistry: death of a myth. Consequences for the statistical treatment of geochemical and environmental data. Environmental Geology 39, 1001-1014.

Reimann C., Filzmoser P., Garrett R., 2005. Background and

threshold: critical comparison of methods of determination. Science of the Total Environment 346, 1-16.

Reimann C., Filzmoser P., Garrett R.G., 2002. Factor analysis applied to regional geochemical data: problems and possibilities. Applied Geochemistry 17, 185-206.

Reis A.P., Sousa A.J., Cardoso Fonseca E., 2001. Soil geochemical prospecting for gold at Marrancos (Northern Portugual). Journal of Geochemical Exploration 73, 1-10. doi: 10.1016/S0375-6742(01)00169-8.

Rudnick R. and Gao S., 2010. Composition of the Continental Crust. In: Holland, H., Turekian, K. (Eds.), Readings of Treatise on Geochemistry. Elsevier, Londan, England, 101-123.

Sadeghi M., Billay A., Carranza E.J.M., 2014. Analysis and mapping of soil geochemical anomalies: Implications for bedrock mapping and gold exploration in Giyani area, South Africa. Journal of Geochemical Exploration 154, 180-193. doi: 10.1016/j.gexplo.2014.11.018.

Sany B.T., Salleh,A., Sulaiman A.H., Mehdinia A., Monazami G.H., 2011. Geochemical Assessment of Heavy Metals Concentration in Surface Sediment of West. 5, 77-81.

Shi G., Teng J., Ma H., Wang D., Li Y., 2018. Metals in topsoil in Larsemann Hills, an ice-free area in East Antarctica: Lithological and anthropogenic inputs. Catena 160, 41-49. doi: 10.1016/j.catena.2017.09.001.

Sinclair A.J., 1974. Selection of threshold values in geochemical data using probability graphs. Journal of Geochemical Exploration 3, 129-149.

Siyako M., Bürkan K., Okay A.İ., 1989. Biga ve Gelibolu Yarımadalarının Tersiyer Jeolojisi ve hidrokarbon olanakları. Türkiye Petrol Jeologları Derneği Bülteni 1, 183-200.

Skoog D., West D., Holler F., Crouch S., 2004. Fundamentals of analytical chemistry, 8th ed. Brooks/Cole-Thomson Learning, Belmont, CA 94002, USA.

Sosa-Rodríguez F.S., Vazquez-Arenas J., Peña P.P., Escobedo-Bretado M.A., Castellanos-Juárez F.X., Labastida I., Lara R.H., 2020. Spatial distribution, mobility and potential health risks of arsenic and lead concentrations in semiarid fine top-soils of Durango City, Mexico. Catena 190, 104540. doi: 10.1016/j.catena.2020.104540.

Sun X., Gong Q., Wang Q., Yang L., Wang C., Wang Z., 2010. Application of local singularity model to delineate geochemical anomalies in Xiong'ershan gold and molybdenum ore district, Western Henan province, China. Journal of Geochemical Exploration 107, 21-29. doi: 10.1016/j.gexplo.2010.06.001.

Sungur A., Soylak M., Ozcan H., 2014. Investigation of heavy metal mobility and availability by the BCR sequential extraction procedure: Relationship between soil properties and heavy metals availability. Chemical Speciation and Bioavailability 26, 219-230. doi: 10.3184/095422914X1414 7781158674.

Sungur A., Soylak M., Özcan H., 2016. Chemical fractionation, mobility and environmental impacts of heavy metals in greenhouse soils from Çanakkale, Turkey. Environmental Earth Sciences 75, 1-11. doi: 10.1007/s12665-016-5268-3.

Sungur A., Soylak M., Yilmaz E., Yilmaz S., Ozcan H., 2015. Characterization of Heavy Metal Fractions in Agricultural Soils by Sequential Extraction Procedure: The Relationship Between Soil Properties and Heavy Metal Fractions. Soil and Sediment Contamination 24, 1-15. doi: 10.1080/15320383.2014.907238.

Sungur A., Vural A., Gundogdu A., Soylak M., 2020. Effect of antimonite mineralization area on heavy metal contents and geochemical fractions of agricultural soils in Gümüşhane Province, Turkey. Catena 184, 104255. doi: 10.1016/j.catena.2019.104255.

Teng Y., Ni S., Wang J., Zuo R., Yang J., 2010. A geochemical survey of trace elements in agricultural and non-agricultural topsoil in Dexing area, China. Journal of Geochemical Exploration 104, 118-127. doi: 10.1016/j.gexplo.2010.01.006.

Vural A., 2020. Investigation of the relationship between rare earth elements, trace elements, and major oxides in soil geochemistry. Environmental Monitoring and Assessment 192, 124. doi: 10.1007/s10661-020-8069-9.

Vural A., 2019. Evaluation of soil geochemistry data of Canca Area (Gümüşhane, Turkey) by means of Inverse Distance Weighting (IDW) and Kriging methods-preliminary findings. Bulletin of the Mineral Research and Exploration 158, 195-216. doi: 10.19111/bulletinofmre.430531.

Vural A., 2018. Relationship between the geological environment and element accumulation capacity of Helichrysum arenarium. Arabian Journal of Geosciences 11, 258. doi: 10.1007/s12517-018-3609-0.

Vural A., 2017. Gold and Silver Content of Plant Helichrysum Arenarium, Popularly Known as the Golden Flower, Growing in Gümüşhane, NE Turkey. Acta Physica Polonica A 132, 978-980. doi: 10.12693/APhysPolA.132.978.

Vural A., 2016. Assessment of Sessile Oak (Quercus petraea L.) Leaf as Bioindicator for Exploration Geochemistry. Acta Physica Polonica A 130, 191-193. doi: 10.12693/APhysPolA.130.191.

Vural A., 2015a. Contamination assessment of heavy metals associated with an alteration area: Demirören Gumushane, NE Turkey. Journal of the Geological Society of India 86, 215-222. doi: 10.1007/s12594-015-0301-9.

Vural A., 2015b. Biogeochemical characteristics of Rosa canina grown in hydrothermally contaminated soils of the Gümüşhane Province, Northeast Turkey. Environmental Monitoring and Assessment 187, 486. doi: 10.1007/s10661-015-4708-y.

Vural A., 2015c. Assessment of metal pollution associated with an alteration area: Old Gümüşhane, NE Black Sea. Environmental Science and Pollution Research 22, 3219-3228. doi: 10.1007/s11356-014-2907-7.

Vural A., 2014. Trace/heavy metal accumulation in soil and in the shoots of acacia tree, Gümüşhane-Turkey. Bulletin of the

Mineral Research and Exploration 148, 85-106.

Vural A., 2006. Bayramiç (Çanakkale) ve Çevresindeki Altın Zenginleşmelerinin Araştırılması. Ankara Üniversitesi.

Vural A. and Aydal D., 2020a. Soil geochemistry study of the listvenite area of Ayvacik (Çanakkale, Turkey). Caspian Journal of Environmental Sciences 18, 205-215.

Vural A. and Aydal D., 2020b. Determination of Lithological Differences and Hydrothermal Alteration Areas by Remote Sensing Studies: Kısacık (Ayvacık-Çanakkale, Biga Peninsula, Turkey). Journal of Engineering Research and Applied Science 9, 1341-1357.

Vural A. and Aydal D., 2016. Using soil geochemistry for gold exploration:Ayvacık (Çanakkale-Northwest Turkey). 34th National and the 2nd International Geosciences Congress. Tehran, Iran.

Vural A., Aydal D., Akpınar İ., 2011. A low sulphur epithermal gold mineralization in Kisacik-Ayvacik area (Çanakkale-Turkey). Mineralogical Magazine 75, 2105.

Vural A. and Çiçek B., 2020. Cevherleşme Sahasında Gelişmiş Topraklardaki Ağır Metal Kirliliği. Düzce Üniversitesi Bilim ve Teknoloji Dergisi 8, 1533-1547. doi: 10.29130/dubited.643775.

Vural A. and Çiçek B., 2019. Heavy Metal Pollution in Developed Soils on Mineralization Zone. 3rd International Conference on Advanced Engineering Technologies (ICADET). Bayburt, Türkiye, 880-884.

Vural A. and Erdoğan M., 2014. Eski Gümüşhane Kırkpavli Alterasyon Sahasında Toprak Jeokimyası. Gümüşhane Üniversitesi Fen Bilimleri Enstitüsü Dergisi 4, 1-15.

Vural A. and Erdoğan M., 2013. İz Bulucu Elementlerden Yararlanarak Toprak Jeokimyası İle Altın Cevherleşmesinin Araştırılması: Kırkpavli, Gümüşhane-Türkiye. 66. Türkiye Jeoloji Kurultayı. Ankara, Türkiye.

Vural A., Kaya S., Başaran N., Songören O.T., 2009. Anadolu Madenciliğinde İlk Adımlar. Maden Tetkik ve Arama Genel Müdürlüğü, MTA Kültür Serisi-3, Ankara, Türkiye.

Vural A. and Şahin E., 2012. Gümüşhane Şehir Merkezinden Geçen Karayolunda Ağır Metal Kirliliğine Ait İlk Bulgular. Gümüşhane Üniversitesi, Fen Bilimleri Enstitüsü Dergisi 2, 21-35.

Wang C., Carranza E.J.M., Zhang S., Zhang J., Liu X., Zhang D., Sun X., Duan C., 2013. Characterization of primary geochemical haloes for gold exploration at the Huanxiangwa gold deposit, China. Journal of Geochemical Exploration 124, 40-58.

Wang Z., Erten O., Zhou Y., Chen J., Xiao F., Hou W., 2017. A spatially weighted singularity mapping method applied to identify epithermal Ag and Pb-Zn polymetallic mineralization associated geochemical anomaly in Northwest Zhejiang, China. Journal of Geochemical Exploration 189, 122-137. doi: 10.1016/j.gexplo.2017.03.017.

Xiong Y., Zuo R., Carranza E.J.M., 2018. Mapping mineral prospectivity through big data analytics and a deep learning algorithm. Ore Geology Reviews 102, 811-817. doi: 10.1016/j.oregeorev.2018.10.006.

Xu S., Hu X., Carranza E.J.M., Wang G., 2020. Multi-parameter Analysis of Local Singularity Mapping and Its Application to Identify Geochemical Anomalies in the Xishan Gold Deposit, North China. Natural Resources Research 29, 3425-3442. doi: 10.1007/s11053-020-09669-5.

Yilmaz H., 2003. Geochemical exploration for gold in western Turkey: Success and failure. Journal of Geochemical Exploration 80, 117-135. doi: 10.1016/S0375-6742(03)00187-0.

Yilmaz H., Sonmez F.N., Carranza E.J.M., 2015. Discovery of Au-Ag mineralization by stream sediment and soil geochemical exploration in metamorphic terrain in western Turkey. Journal of Geochemical Exploration 158, 55-73. doi: 10.1016/j.gexplo.2015.07.003.

Yusta I.N., Velasco F., Herrero J.M., 1998. Anomaly threshold estimation and data normalization using EDA stastistics: Application to lithogeochemical exploration in lower cretaceous Zn-Pb carbonate-hosted deposits, Northern Spain. Applied Geochemistry 13, 421-439.doi: 10.1016/S0883-2927(97)00095-4.

Zhang S., Carranza E.J.M., Xiao K., Chen Z., Li N., Wei H., Xiang J., Sun L., Xu Y., 2021. Geochemically Constrained Prospectivity Mapping Aided by Unsupervised Cluster Analysis. Natural Resources Research 30, 1955-1975. doi: 10.1007/s11053-021-09865-x.

Zuo R. and Wang J., 2015. Fractal/multifractal modeling of geochemical data: A review. Journal of Geochemical Exploration.doi: 10.1016/j.gexplo.2015.04.010.

Zuo R., Wang J., Chen G., Yang M., 2015. Identification of weak anomalies: A multifractal perspective. Journal of Geochemical Exploration 148, 12-24. doi: 10.1016/j.gexplo.2014.05.005.